

Automatic object detection for disassembly and recycling of electronic board components

Original

Automatic object detection for disassembly and recycling of electronic board components / Puttero, Stefano; Nassehi, Aydin; Verna, Elisa; Genta, Gianfranco; Galetto, Maurizio. - ELETTRONICO. - 127:(2024), pp. 206-211. (Intervento presentato al convegno 10th CIRP Conference on Assembly Technology and Systems (CIRP CATS 2024) tenutosi a Karlsruhe nel 24-26 Aprile 2024) [10.1016/j.procir.2024.07.036].

Availability:

This version is available at: 11583/2993379 since: 2024-10-14T08:07:02Z

Publisher:

Elsevier

Published

DOI:10.1016/j.procir.2024.07.036

Terms of use:

This article is made available under terms and conditions as specified in the corresponding bibliographic description in the repository

Publisher copyright

(Article begins on next page)

10th CIRP Conference on Assembly Technology and Systems (CIRP CATS 2024)

Automatic object detection for disassembly and recycling of electronic board components

Stefano Puttero^{a,*}, Aydin Nassehi^b, Elisa Verna^a,
Gianfranco Genta^a, Maurizio Galetto^a

^aDepartment of Management and Production Engineering, Politecnico di Torino, Corso Duca degli Abruzzi 24, 10129 Torino, Italy

^bDepartment of Mechanical Engineering, University of Bristol, Queens Building, University Walk, Bristol, BS8 1TR, United Kingdom

* Corresponding author. Tel.: +39 011 0907236; E-mail address: stefano.puttero@polito.it

Abstract

This paper presents the development of a deep learning-based object recognition system designed to automate and speeding up the disassembly process of electrical and electronic components. The main goal is to address the mounting global issue of Waste Electrical and Electronic Equipment (WEEE) management. The increasing availability of technology and the expansion of consumer markets have led to a significant surge in the generation of WEEE, necessitating the urgent development of sustainable and automated strategies for its disposal and resource recovery. Traditional manual disposal methods and the uncontrolled accumulation of WEEE can pose serious threats to the environment, human health and natural resources. A comprehensive approach, involving advanced recycling technologies, life-cycle management and policy reforms is required to handle this escalating waste stream.

The complexity of WEEE management is heightened by the diversity of product design and composition, making efficient material selection processes often labour-intensive and expensive. This work focuses on the automated detection and sorting of WEEE products. The proposed system enables rapid identification of products and components, in order to facilitate the subsequent disassembly and reuse of components that are still considered functional, safe, and of good quality. This concept is illustrated through a case study where recognition of six different electronic boards is performed.

© 2024 The Authors. Published by Elsevier B.V.

This is an open access article under the CC BY-NC-ND license (<https://creativecommons.org/licenses/by-nc-nd/4.0>)

Peer-review under responsibility of the scientific committee of the 18th CIRP Conference on Computer Aided Tolerancing

Keywords: Object detection; Vision system; Disassembly; WEEE recycling

1. Introduction

In recent years, the proliferation of waste electrical and electronic equipment (WEEE) has created an unprecedented global challenge. The rapid technological advancement of today's market has led to a dramatic escalation of the WEEE generation rate (estimated increase of 3-5% per year), driving the need for effective and sustainable alternative waste management strategies [1]. Among these strategies, the role of deep learning is emerging as a crucial alternative that can revolutionise the disassembly and recycling processes of WEEE.

WEEE, also known as e-waste, covers a wide range of electronic equipment, from consumer electronics to complex computer and communications systems. This heterogeneous waste stream presents complex challenges due to the varying composition of the materials to be handled, the integration of different types of components and the presence of dangerous substances [2]. Traditional WEEE management methods often involve manual and semi-automated processes that are not only time, cost and labour intensive, but also prone to inefficiency and inaccuracy. As a result, managing this growing waste stream requires a comprehensive approach that takes into account the entire product life cycle [3].

Deep learning, a subset of machine learning, has become a paradigm shifter in several industries, demonstrating outstanding capabilities in object detection, natural language processing and pattern recognition [4]. Also in the WEEE sector, researches have shown how neural networks trained on big data have great potential for WEEE recognition, sorting and disassembly [5]. By enabling precise identification and separation of materials, the application of deep learning to WEEE promises to increase the efficiency of disassembly and subsequent recycling of electronic components.

The main goal of this paper is to present an application of a convolutional neural network (CNN) in the efficient recognition of electronic components. By harnessing the power of neural networks, this study seeks to explore new approaches that can be used for automatic component recognition and material classification. Through the experimental results, this paper aims to demonstrate the tangible benefits of integrating deep learning methods in the field of WEEE management.

2. Object detection using convolutional neural networks

2.1. Convolutional neural network architecture

Object detection is a computer vision activity that detects instances of objects of a given class in digital images. The goal of object detection is to develop computational models that indicate which objects are present in an image and where they are located [6]. Among the various techniques, CNN is certainly the most widely used for object detection. A CNN is a hierarchical category of deep neural networks designed to process and extract features from images [7]. This hierarchical structure is characterised by multiple layers, each consisting of interconnected units called neurons [6]. The innovation of CNNs lies in the use of convolutional layer, which use adaptive filters to perform localised convolutions on the input data, capturing distinctive features and patterns within the visual domain. Subsequent pooling layer reduce spatial dimensions while preserving essential information, promoting translation invariance and enabling feature extraction [6]. Feature classification takes place in the fully connected layer, where all the features extracted from the previous layers converge. Finally, the output layer, consisting of a number of neurons equal to the number of classes detected, shows the results of the classification. This intricate interplay between the convolutional and pooling layers gives CNNs the ability to learn increasingly abstract and complex features automatically and adaptively from the raw data [7]. Fig. 1 shows the schematic diagram of a basic CNN.

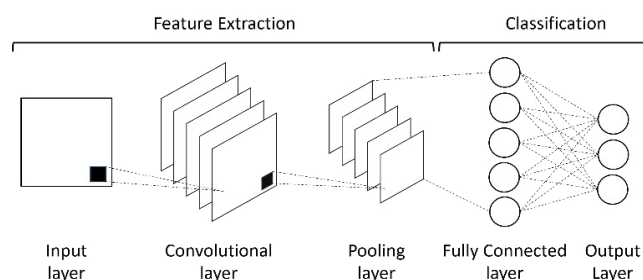


Fig. 1. Schematic diagram of a basic CNN architecture. Adapted from [8].

The operation of a CNN is based on the concept of bounding boxes. Each object identified is enclosed by a bounding box and marked by a score that indicates the model's confidence in associating the box with a real object instance. Accordingly, the confidence score quantifies the probability that the bounding box precisely encapsulates a detected object [6].

In the field of CNNs, their architecture can be classified into two different paradigms: one-stage CNNs and two-stage CNNs [4,7]. One-stage CNNs, often referred to as single-strike detectors, simplify the process by directly predicting object classes and bounding boxes in a single pass through the network. This fast approach reduces computational complexity and inference time, making it suitable for real-time applications [6]. This category includes the YOLO (You Only Look Once) models [9]. In contrast, two-stage CNNs consist of a preliminary stage that generates regions of interest (ROIs), followed by a stage for object classification and localisation. While introducing an additional layer, two-stage CNNs tend to produce more precise prevision. Neural networks such as the Regional proposal with Convolutional Neural Network (R-CNN) and Faster R-CNN fall into this category [9]. The trade-off between speed and precision defines the distinction between the two paradigms: one-stage CNNs favour efficiency and real-time operation, while two-stage CNNs favour precision and adaptability. The choice between the two paradigms depends on the specific requirements of the application and the balance between real-time constraints and the desired quality of sensing [7].

2.2. Convolutional neural networks for WEEE

Numerous researches have highlighted the capabilities of neural networks, particularly CNNs, when trained on large datasets for WEEE management [10,11]. The potential of these neural networks is crucial in overcoming the persistent problems of low recall and precision associated with conventional recognition methods [10].

Even for WEEE, the choice of the most suitable neural network depends on the application. According to Xu et al. [10], if high precision is required in detecting electronic components, two-stage networks should be used. On the other hand, if the application requires real-time component recognition, a single-stage neural network is more suitable [11]. Considering that the neural network will be used in the real-time recognition of electronic boards and their subsequent disassembly (see Section 5), a model based on the YOLOv5 paradigm has been developed.

3. Research framework

As above mentioned, methods for inspecting printed circuit boards are well-established in both academic literature and industry practice [5,12]. However, these methods typically rely on the assumption that electronic components are fixed in position on the board. In contrast, the proposed case study shows an innovative method for detecting components on the assembled electronic boards with variable positions (see Section 4). Fig. 2 illustrates the WEEE management stages where the proposed automatic recognition system is applied.

The system first identifies individual components; then, it determines the board's type and function, significantly reducing potential human errors in these critical recognition steps (highlighted by the red box). This advancement sets the stage for automated board disassembly and the subsequent reuse or recycling of functional components, as it will be discussed in Section 5.

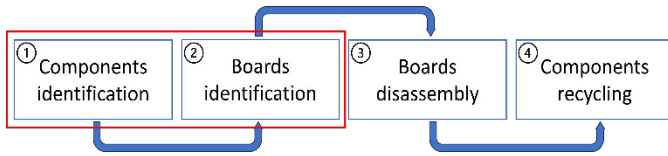


Fig. 2. Stages of Electronic Board Processing for WEEE Management.

Building on the automatic recognition capabilities outlined in Fig. 2, this paper delves into the application of the YOLOv5 algorithm within WEEE management systems. YOLOv5's proficiency in detecting and locating multiple objects in images makes it particularly suited to the intricacies of WEEE management, where rapid and accurate identification of electronic waste components is crucial. By applying YOLOv5 to identify components on electronic boards without fixed positions, a notable enhancement can be obtained in the efficiency and effectiveness of sorting, recycling and disposal processes [11]. The case study affirms that incorporating YOLOv5 into WEEE management systems fosters a more sustainable approach to e-waste management (see the next section).

4. Case study

4.1. ARDUINO boards

Six different electronic boards (named from “pA” to “pF”) from the ARDUINO® UNO starter kit were selected as a case study. The ARDUINO UNO starter kit consists of three main elements: the microcontroller, the components (e.g., wires, buttons, resistors, etc.) and the breadboard, which is used as the basis for building different product variants. The characteristics of the selected electronic boards are reported in Table 1 [13].

Table 1. Characteristics of the six electronic boards (pA-pF).

	pA	pB	pC	pD	pE	pF
Button	-	2	4	-	2	1
H-Bridge	-	-	-	-	1	-
LCD	-	-	-	-	-	1
LED	1	1	-	1	-	-
Photoresistor	-	-	-	3	-	-
Piezo	-	-	1	-	-	-
Potentiometer	-	-	-	-	1	1
Resistor	1	1	4	6	2	2
Wire	1	4	7	11	15	17
N° of parts	3	8	16	21	21	22

This type of product allows different types of electronic boards to be assembled using the same initial components. If

one of the product variants does not work properly, it is possible to disassemble the product itself and reuse the still-working components to produce a new variant. Moreover, no soldering is required, as the ARDUINO breadboard is made up of rows and columns of holes that transfer electricity through the connections [13]. Thus, ARDUINO boards can simulate the assembly and disassembly processes of a Printed Circuit Board (PCB), which is the core component of many electronic products [11,13], eliminating the challenges associated with soldering. Fig. 3 shows two examples of electronic boards.

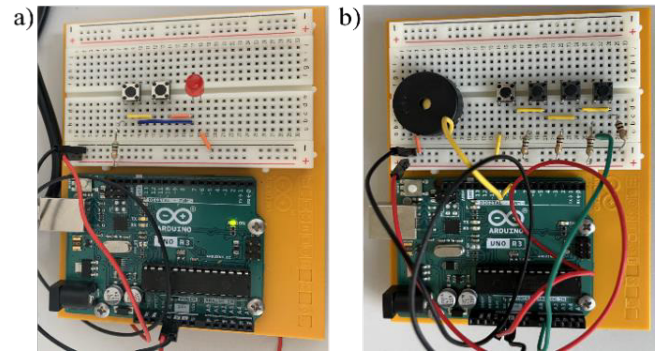


Fig. 3. Example of assembled electronic boards: (a) pB and (b) pC.

Despite their distinct functions and varying levels of customization, which range from simple to more complex [13], these six boards share a key commonality: they consist of similar, unsoldered components, which makes them potentially reusable (if functioning). This characteristic is especially significant in the context of real-world product design, where a wide range of products frequently employ similar and interchangeable elements.

4.2. Dataset generation

YOLOv5 offers faster real-time object detection and higher precision than other deep learning algorithms. Training a YOLOv5 model requires darknet format images, i.e., images in which each component is labelled and contained within bounding boxes. In this case study, the dataset for training, testing and validation was imported directly from Roboflow [14].

The first step was to upload the initial 240 images, i.e., 40 images for each of the six product types, to the Roboflow website. During the tests, it was found that using at least 40 different images per product allowed the network to extract more robust information. To reduce the noise generated in the neural network, the 240 images were cropped with a focus on the breadboard (see Fig. 4). Afterwards, an initial phase of image labelling was carried out, indicating the individual bounding boxes of the recognised components. The labelling was performed manually using Roboflow's Smart Polygon tool to ensure high precision of prediction [14]. At the end of this first phase, 9 different classes (i.e., button, H-bridge, LCD, LED, photoresistor, piezo, potentiometer, resistor, wire) were identified. All the 240 images were resized to 416x416 pixels. Before the training phase, Roboflow allows data augmentation to increase the size of the initial dataset [14]. In this study, several data augmentation such as flipping (horizontal and

vertical), rotation (between -20° and $+20^\circ$), saturation (between -50% and $+50\%$) and zoom (between -20% and $+20\%$) were applied to the initial images (see Fig. 4).

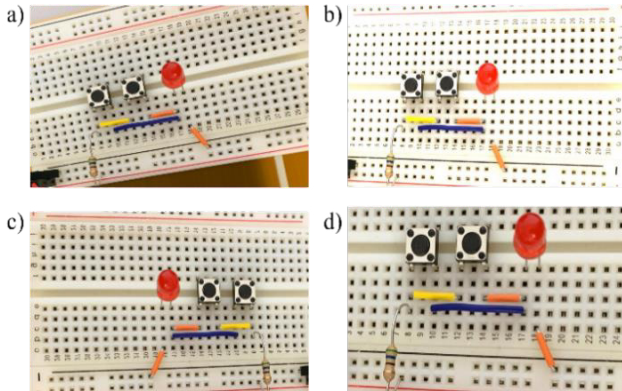


Fig. 4. Example of data augmentation applied to pB images: (a) -20° rotation, (b) $+20\%$ brightness, (c) horizontal flip, and (d) $+20\%$ zoom.

The final dataset size amounted to 728 images. This dataset was used to train, validate and test the YOLOv5 network. Specifically, 80% of the dataset was used for the training phase and the remaining 20% for the validation and testing phases. In this case study, the YOLOv5 network was trained from scratch using the above-described database.

4.3. Network training

Google Colab, a research project for prototyping machine learning models on powerful hardware options such as GPUs and TPUs, was used to implement the YOLOv5 network. This platform provides a Jupyter notebook environment for interactive development without the need for high-performance local resources [15]. Among the various GPUs, CPUs and TPUs offered by Google Colab, the NVIDIA T4 GPU was selected. With 16GB of RAM, this GPU excels at parallel processing, making it ideal for training deep learning models.

In the first phase of neural network training, the YOLOv5 repository was downloaded from the ultralytics GitHub profile [16]. This repository contains the pre-written Python files for training, validation and testing and the four different variants of the YOLOv5 models: s, m, l and x [7]. Given the small size of the dataset and the need for real time recognition, the YOLOv5s model was selected. The database link was downloaded from the Roboflow website and training began by feeding the dataset into the custom YOLOv5s model. At this early stage, it was crucial to define the correct number of epochs (i.e. the number of times the algorithm runs through the entire training data set) and batches (i.e. the number of samples to be processed before updating the internal model parameters) [4]. In this case study, the number of epochs was set to 200 and the number of batches to 32. These values were determined by observing the learning performance and comparing this number with the model's error rate to find the best balance between training time and performance. Training was performed using the Python training file in the downloaded repository, and the best weights were saved and used to detect components when training was complete. The process took almost an hour.

5. Results and discussions

5.1. Performance metrics

Object detection methods use several criteria to evaluate detector performance, such as precision, recall and mean average precision. All these criteria are based on the concept of Intersection of Union (IoU), i.e. the ratio of the overlap area to the union area between the ground truth (actual object position) and the predicted bounding box [17]. The IoU measures the spatial alignment between the predicted and actual positions of objects and provides an index of location precision. In common practice, a predefined threshold is used along with the IoU metric to assess the precision of the predictions. If the IoU exceeds this threshold, a True Positive (TP) is established, indicating that the model has correctly classified the object. Conversely, if the IoU falls below the threshold, three different scenarios can occur: (i) False Positive (FP), i.e. the model identifies an object that does not match the ground truth; (ii) False Negative (FN), i.e. the model does not identify an object that exists in the ground truth; (iii) True Negative (TN), i.e. the model does not identify an object that does not appear in the ground truth. [17]. These metrics (TP, FP, TN and FN) are counts that give an indication of the model predictive ability.

Precision involves the model's capacity to exclusively recognize pertinent objects, quantified as the ratio of positive predictions. A high precision means that the model is making fewer FP errors. On the other hand, recall concerns the model's capability to locate all relevant instances. It measures the proportion of positive predictions in relation to the total number of ground truths bounding boxes. Accordingly, precision and recall can be defined as [17,18]:

$$Precision = \frac{TP}{TP+FP}, \quad (1)$$

$$Recall = \frac{TP}{TP+FN}. \quad (2)$$

There is often a trade-off between precision and recall. Increasing one metric may lead to a decrease in the other metric. A good object detection model has high precision and recall at a suitable decision threshold. To study the joint performance of precision and recall, it is usual to create the precision-recall curve (P(R) curve) and calculate the area under the curve [18]. The area under this curve represents the Average Precision (AP) of the recognition model and can be defined as:

$$AP = \int_0^1 P(R) dR. \quad (3)$$

Each class identified by the model (nine in our case study, see Section 4.2) has its AP value. The mean average precision (mAP), which is one of the best measures of model precision, is obtained by averaging the AP values of the different classes. As a result, the mAP can be calculated as follows:

$$mAP = \frac{1}{N} \sum_{i=1}^N AP_i, \quad (4)$$

where N is the total number of classes and AP_i is the average precision in the i -th class [17,18]. It is noteworthy how AP_i values depend on the value of the defined IoU threshold (since precision and recall depend on this threshold). Therefore, to avoid this ambiguity, it is important to assess the mAP using a different set of thresholds. It is common practice to consider mAP defined with IoU equal to 0.5 (mAP_0.5) and all mAP values with IoU between 0.5 and 0.95 with a step of 0.05 (mAP_0.5:0.95).

5.2. Results

Fig. 5 shows the results of training and validation sets of the YOLOv5s model. The graphs highlight the most important criteria to evaluate detector performances: loss, precision, recall and mAP. In particular, Fig. 5(a-f) reports the three components of the loss function over epochs: box loss, objectness loss and classification loss. Box loss indicates how well the model can locate the centre of an object and how much the predicted bounding box covers an object. Objectness loss measures the probability that an object is present in a proposed region of interest. If objectness is high, the image window is likely to contain an object. Classification loss refers to the ability of the algorithm to predict the correct class of an object. For all three types of losses, the lower the loss, the better the model's performances. Over epochs, Fig. 5(a-f) shows that all three loss categories have a decreasing trend towards zero for both the validation and training sets. This trend is an indicator of the model's ability to correctly detect electronic components.

Regarding precision, recall and mAP, the values gained by the model are reported in the first row of Table 2. The same results can be seen graphically in Fig. 5(g-l), where an increasing trend towards unit value can be observed. The analysis leads to a mAP of 94.5%, which indicates a good capability of the model to detect components a good capability of the model to detect components. This capability is also reflected in the individual component classes in Table 2, detailing the precision, recall and mAP values for each of the

identified electronic components. For all 9 classes, the model shows very high performance, confirming the loss analysis. Some restrictions apply only to wire and resistor classes, as for more complex products (pE, pF) there is often an overlap between wire and resistor, making identification more difficult.

Table 2. YOLOv5s model results.

Classes	Precision	Recall	mAP0.5	mAP0.5:0.95
All	0.911	0.940	0.945	0.794
Button	0.985	1	0.995	0.895
H-Bridge	0.853	1	0.995	0.995
LCD	0.911	1	0.995	0.808
LED	1	0.985	0.995	0.911
Photoresistor	0.812	0.889	0.949	0.821
Piezo	0.852	1	0.898	0.726
Potentiometer	1	0.982	0.995	0.796
Resistor	0.828	0.705	0.760	0.499
Wire	0.961	0.896	0.919	0.699

Upon validating the model's performance on the dataset, the testing phase was performed. The testing part of the database was fed into the network, requesting as output the product images with their respective labels for each component. Within a few seconds, the model processed the different images, assigning each detected component a detect box with the confidence level of detection. The model produced the outputs shown in Fig. 6, representing the detections for product pB and product pC. Fig. 6 shows that each detected electronic component is surrounded by a differently coloured detection box (one for each class) marked by a confidence level of detection. For the majority of the electronic components, this detection level approaches 90%, underscoring the high detection capability of the implemented model. This result suggests that the developed system is highly reliable and holds promise for future applications.

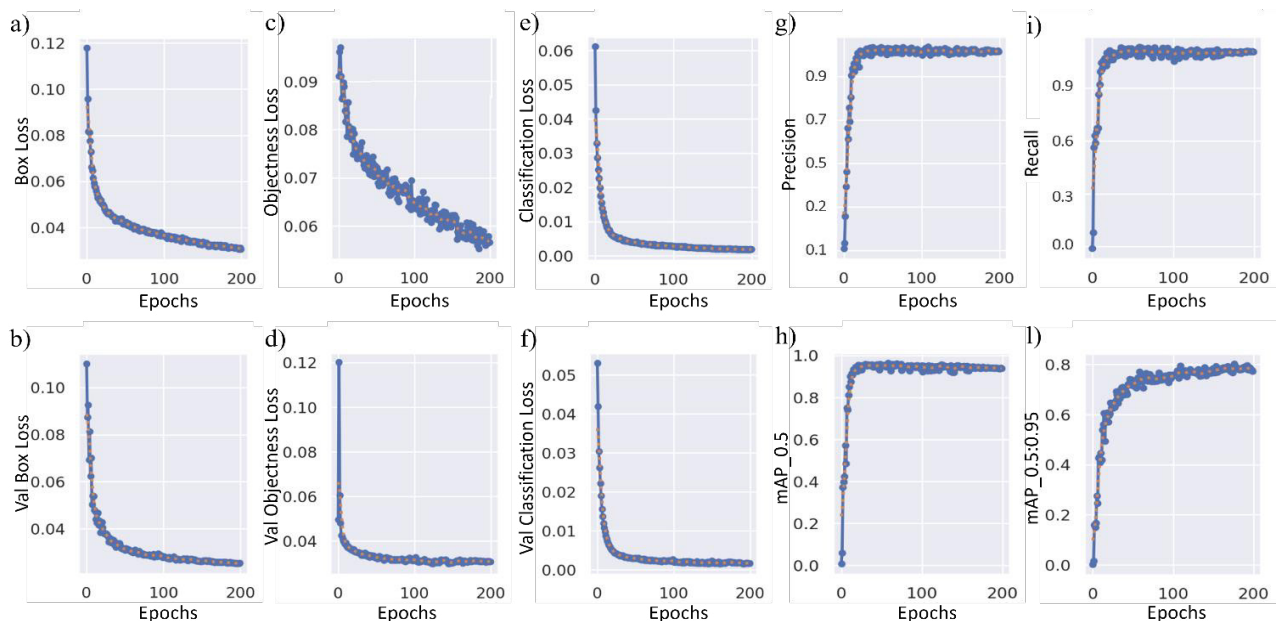


Fig. 5. Plotting of: a-b) training and validation box loss; c-d) training and validation objectness loss; e-f) training and validation classification loss; g) precision; h) mAP_0.5; i) recall and l) mAP-0.5:0.95.

After testing, the detected information was used to develop a classification system for electronic boards. Based on the number and type of components identified, the system is able to classify different electronic boards. For example, considering product pB in Fig. 6(a), the system identifies 4 wires, 1 resistor, 2 buttons and 1 LED. Comparing the recognised components and the available circuit boards (pA-pF), the only board with these characteristics is the product pB. Consequently, the system labels this image as pB. This is useful in scenarios where multiple products made up of the same components need to be identified (see Section 6).

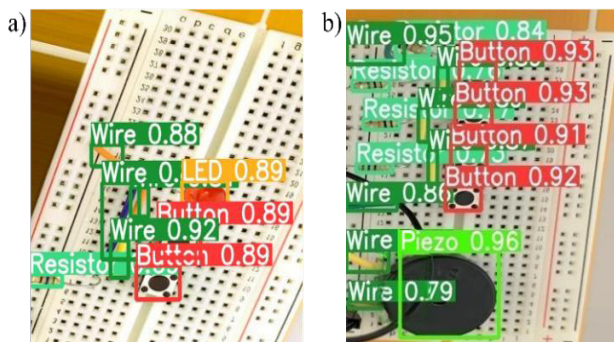


Fig. 6. Electronic components prediction for (a) pB and (b) pC.

Finally, Fig. 6 and Table 2 show the ability of the model to detect electronic components in real time. In particular, the system can process and classify an image every 0.72 seconds, making it ideal for production line use. The system also proved effective and reliable in uncontrolled environments such as the laboratory. For example, by recognising the components present, the automatic recognition system classifies the board type and signals if one or more components are missing. The system also performed well in the case of poorly positioned components or dirt on the board (provided that this does not compromise the minimum visibility required by the camera).

6. Conclusions and future works

The relentless proliferation of technology and consumer markets has led to an exponential increase in the generation of WEEE. This increase not only poses environmental challenges, but also underlines the urgent need for sustainable approaches to facilitate disposal and potential recovery of valuable resources. The complexity of this problem requires innovative solutions that go beyond traditional methods. Leveraging the capabilities of deep learning technology, an innovative recognition system has been developed to simplify the process of dismantling electronic components.

The aim of this paper is to implement an innovative object recognition system for identifying electronic products. The feasibility of this approach is highlighted by an illustrative case study showing the identification of electronic components from six different electronic boards. In particular, the efficient real-time detection of electronic components and ARDUINO boards was demonstrated using a YOLOv5s neural network application. The experimental findings not only validate the feasibility of the proposed system, but also provide a powerful

insight into its potential to innovate WEEE management methods on a larger scale, beyond the limits of the preset positions of the electronic components within the board.

Although this study is a first step towards innovative WEEE management, further research is needed to refine the scalability and applicability of the system to a broader range of electronic components. Future work includes refining and increasing the size of the initial database in order to apply the recognition system in a Human-Robot Collaboration (HRC) environment for the disassembly of electronic boards. Thanks to the implemented YOLOv5s model, a cobot equipped with a camera could identify the different ARDUINO boards and perform a customised disassembly for each electronic board. As a result, the human operator could be guided step-by-step by the cobot's movements through the disassembly process and subsequent testing phase, tailored to the specific board identified. This collaboration could lead to a standardised disassembly process, reducing variability and streamlining the identification and extraction of functional components.

References

- [1] Shittu OS, Williams ID, Shaw PJ. Global E-waste management: Can WEEE make a difference? A review of e-waste trends, legislation, contemporary issues and future challenges. *Waste Manag* 2021;120:549–63.
- [2] Zhang L, Geng Y, Zhong Y, Dong H, Liu Z. A bibliometric analysis on waste electrical and electronic equipment research. *Environ Sci Pollut Res* 2019;26:21098–108.
- [3] Wang L, Wang XV, Gao L, Váncaza J. A cloud-based approach for WEEE remanufacturing. *CIRP Ann* 2014;63:409–12.
- [4] Zhao Z-Q, Zheng P, Xu S-T, Wu X. Object Detection With Deep Learning: A Review. *IEEE Trans Neural Networks Learn Syst* 2019;30:3212–32.
- [5] Nowakowski P, Pamula T. Application of deep learning object classifier to improve e-waste collection planning. *Waste Manag* 2020;109:1–9.
- [6] Zou Z, Chen K, Shi Z, Guo Y, Ye J. Object Detection in 20 Years: A Survey. *Proc IEEE* 2023;111:257–76.
- [7] Dhillon A, Verma GK. Convolutional neural network: a review of models, methodologies and applications to object detection. *Prog Artif Intell* 2020;9:85–112. <https://doi.org/10.1007/s13748-019-00203-0>.
- [8] Phung, Rhee. A High-Accuracy Model Average Ensemble of Convolutional Neural Networks for Classification of Cloud Image Patches on Small Datasets. *Appl Sci* 2019;9:4500.
- [9] Sultana F, Sufian A, Dutta P. A Review of Object Detection Models based on Convolutional Neural Network. *Image Process. Based Appl., Springer Singapore*; 2019.
- [10] Xu Y, Yang G, Luo J, He J. An Electronic Component Recognition Algorithm Based on Deep Learning with a Faster SqueezeNet. *Math Probl Eng* 2020;2020:1–11.
- [11] Adibhatla VA, Chih H-C, Hsu C-C, Cheng J, Abbod MF, Shieh J-S. Applying deep learning to defect detection in printed circuit boards via a newest model of you-only-look-once. *Math Biosci Eng* 2021;18:4411–28.
- [12] SPEA. <https://www.spea.com/it/> (accessed December 17, 2023).
- [13] Verna E, Puttero S, Genta G, Galetto M. Exploring the Effects of Perceived Complexity Criteria on Performance Measures of Human–Robot Collaborative Assembly. *J Manuf Sci Eng* 2023;145:101014.
- [14] Roboflow. <https://roboflow.com/> (accessed August 14, 2023).
- [15] Bisong E. Google Colaboratory. *Build. Mach. Learn. Deep Learn. Model. Google Cloud Platf., Berkeley, CA: Apress*; 2019, p. 59–64.
- [16] Github. <https://github.com/ultralytics/yolov5> (accessed August 14, 2023).
- [17] Zaidi SSA, Ansari MS, Aslam A, Kanwal N, Asghar M, Lee B. A survey of modern deep learning based object detection models. *Digit Signal Process* 2022;126:103514.
- [18] Gong H, Mu T, Li Q, Dai H, Li C, He Z, et al. Swin-Transformer-Enabled YOLOv5 with Attention Mechanism for Small Object Detection on Satellite Images. *Remote Sens* 2022;14:2861.